Deposition of ZnO/α-F_2O_3 Nanocomposites on Screen-Printed Electrodes for Electrochemical Arsenic Detection

Sreymean Ngok [1]
https://orcid.org/0009-0003-2867-1754
sreymean.ngok@liu.se

Magnus Willander [1]
https://orcid.org/0000-0001-6235-7038

Omer Nur [1]
https://orcid.org/0000-0002-9566-041X

Abstract

Developing a robust screen-printed electrochemical sensor for the determination of As^{5+} in drinking water based on metal oxide nanocomposite is still a challenging task. In this article, the development of electrochemical sensors by using ZnO/α-Fe_2O_3 nanoparticles (NPs) deposited on a screen-printed carbon electrode (SPCE) for As^{5+} detection is presented. The SPCE was modified by drop casting of ZnO NPs and α-Fe_2O_3NPs on the SPCE and used as a working electrode. This electrode was analysed for different concentrations of α-Fe_2O_3NPs and ZnO NPs. The samples were denoted 2.5 wt% F, 5 wt% F, 7.5 wt% F, 2.5 wt% Z, 5 wt% Z and 7.5 wt% Z, depending on the weight percentage of the NPs. The properties of the nanocomposite were characterised by UV-vis, FESEM and XRD. Moreover, the electrochemical characteristics were also analysed via linear sweep voltammetry in different water solutions with a wide range of arsenic concentrations from 0 to 50 µg/L. The results were analysed for different concentrations of both of the NPs. The best performance sample was then identified and used for further analysis. From the electrochemical studies, the sensor attained a low detection limit of 2.7 ppb for As^{5+}, which is below the maximum allowable limit recommended by the World Health Organization for standard drinking water. Consequently, the results confirm that the electrochemical catalytic activity of ZnO/α-Fe_2O_3NPs/SPCE with 2.5 wt% ZF can be used as an efficient electrode to further develop an As^{5+} sensor system for analysis of real samples.

Keywords: screen-printed electrode; ZnO/α-Fe_2O_3NPs/SPCE (2.5 wt% ZF) electrode; arsenic detection; drinking water

1 Departments of Science and Technology, Physics, Electronics and Mathematics, Linköping University, Sweden.

UNISA university of south africa PRESS

Nano-Horizons
Volume 4 | 2025 | 15 pages

https://doi.org/10.25159/3005-2602/20057
ISSN 3005-2602 (Online)

1 Introduction

Arsenic (As) is a highly toxic element that is found in many different mineral compounds [1]. Arsenic presence in drinking water is considered a serious form of pollution that cause health problems in humans [2], [3]. Most of the toxic arsenic is found in groundwater, which contaminates drinking water in many different countries [4]–[6]. There are many arsenic compounds such as As^{3+}, As^{5+} and As^{0} that are present in the environment and biological systems. As^{3+} or As^{5+} are commonly investigated in the water in the form of inorganic species, which occur as arsenate ($H_2AsO_4^-$ and $HAsO_4^{2-}$) and arsenite (H_3AsO_3) ions as the dominant species in drinking water [7], [8]. The World Health Organization (WHO) has therefore recommended that the maximum allowed contamination level for healthy drinking water is from 50 to 10 ppb [9]. Various analytical techniques, such as hydride generation atomic absorption spectrometry or atomic fluorescence spectrometry[10], inductively coupled plasma-optical emission spectrometry, inductively coupled plasma-mass spectrometry and colorimetric approach [11], can all be used to detect low concentrations of arsenic accurately. Although some of the above-mentioned techniques have detected arsenic effectively, there are some drawbacks for using such techniques. These drawbacks include the need for large, expensive and sophisticated instruments, highly trained operators and extensive sample preparation, which can hinder field and on-site detection of arsenic [10], [12], [13].

Screen-printing techniques are popular for the realisation of electrodes [7], [14], [15]. The screen printing comprises automated manufacturing techniques, which allow the production of less expensive (low cost), small size and robust sensors with good reproducibility, and suitability and the possibility of implementing portable analytical units for on-site control [16], [17]. A route to achieve low-cost mass production of electrodes is through screen printing on flexible substrates. Screen-printed electrodes have been used for the detection of different elements in a variety of samples [18], [19]. However, electrochemical sensor applications of bare screen-printed electrodes have been challenging because of the poor electron transfer and passive charge transfer properties. Owing to these problems, modifications of the bare screen-printed carbon electrodes (SPCEs) by using nanocomposite materials will improve the available electroactive surface area, and increase the porosity and conductivity of the sensing electrodes [17], [20].

To date, metal oxides have been used as sensing materials, for example, cobalt oxide (Co_3O_4), copper oxide (CuO), zinc oxide (ZnO), titanium dioxide (TiO2) and iron oxide (α-Fe_2O_3) [19], [21]. ZnO/α-Fe_2O_3 has been used to detection various materials through the development of electrochemical sensors [17], [22]–[24]. The ZnO/α-Fe_2O_3 nanocomposite, which was used in this study, was prepared through different techniques in many studies [25]–[27]. However, although ZnO/α-Fe_2O_3 has been extensively studied for various applications, there are no reports on screen-printed electrochemical sensors based on ZnO/α-Fe_2O_3 nanocomposites for As^{5+} detection.

In this study, we demonstrate the development of electrochemical sensors by using ZnO/α-Fe_2O_3NPs on SPCEs for As^{5+} detection in drinking water. We fabricated the screen-printed electrochemical sensors for As^{5+} detection in drinking water based on ZnO/α-Fe_2O_3NPs/SPCE (ZF). The SPCEs were modified by drop casting ZnO NPs and α-Fe_2O_3NPs. Analytical, structural and optical characterisation tools have been used to investigate the different properties of the drop-casting nanocomposite materials. The electrochemical performance of the sensor towards As^{5+} detection was investigated by using linear sweep voltammetry (LSV). The detection performance of the ZnO/α-Fe_2O_3NPs/SPCE (ZF) electrode showed promising results and can further be developed as an excellent candidate for the detection of As^{5+} in drinking water.

2 Experiments

2.1 Materials

The chemicals used in this experiment were purchased from Sigma Aldrich and were of analytical grade. The materials were ZnO powder (particles size < 100 nm), α-Fe_2O_3NPs powder (particles size < 50 nm), sodium carboxymethyl cellulose, arsenic standard solution, and potassium hydroxide (KOH). Potassium chloride (KCl), silver nitrate ($AgNO_3$), cadmium nitrate tetrahydrate (Cd $(NO_3)_2$ $4H_2O$), zinc nitrate hexahydrate (Zn $(NO_3)_2 \cdot 6H_2O$) and iron (III) nitrate nonahydrate (Fe $(NO_3)_3 \cdot 9H_2O$) were employed to provide K^+, Ag^+, Cd^{2+}, Zn^{2+} and Fe^{3+} ions correspondingly. All solutions used in the experiments were prepared with deionised water.

2.2 Preparation for ZnO NPs Ink

The ink formula of the working electrode was made from a mixture of 3% (w/w) sodium carboxymethyl cellulose and ZnO powder (particles size < 100 nm) and three different concentrations of 2.5 wt%, 5 wt% and 7.5 wt% were prepared using 20 mL of deionised water. The solutions were stirred for a whole night to obtain consistent ZnO NPs ink.

2.3 Preparation for α-Fe_2O_3NPs Ink

The α-Fe_2O_3 ink was formulated from a mixture of 3% (w/w) sodium carboxymethyl cellulose and α-Fe_2O_3NPs powder (particles size < 50 nm) at three different concentrations of 2.5 wt%, 5 wt% and 7.5 wt% into 20 mL of deionised water. The solutions were stirred for a whole night to obtain consistent α-Fe_2O_3 ink.

2.4 Fabrication of Screen-Printed Carbon Electrodes

The SPCE was attached to the top of a polyethylene naphthalate (PEN) substrate. The conductive ink was applied on top of the PEN substrate by using the screen-printing process. First, the PEN substrate was cleaned with ethanol and put into an ultraviolet (UV) cleaner for 15 minutes. Carbon ink was then applied onto the PEN substrate to form a counter electrode (CE) and working electrode (WE) and dried for 10 minutes. Silver ink was then applied as a reference electrode (RE). Then α-Fe_2O_3 ink and ZnO

ink were applied to the WE by using 4 µL by drop casting and dried at 30 °C for 10 minutes. The samples were denoted 2.5 wt% F, 5 wt% F, 7.5 wt% F, 2.5 wt% Z, 5 wt% Z and 7.5 wt% Z. Finally, α-Fe_2O_3NPs ink was deposited onto the ZnO NPs to obtain ZnO/α-Fe_2O_3NPs/SPCE after analysis of all the samples. The best sample was identified and used further for the electrochemical sensing experiments. See the diagram in Figure 1.

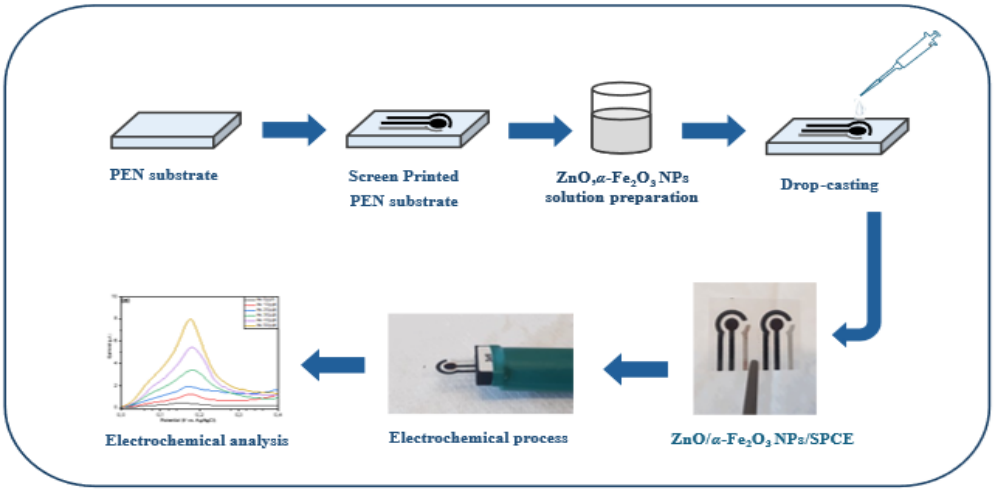

Figure 1: The process for screen printing of the ZnO/ NPs/SPCE electrode on a PEN substrate followed by drop casting and sensing of As^{5+} by LSV

2.5 General Characterisation Techniques

The morphology of all samples was characterised by a field emission scanning electron microscope (FESEM, Sigma 500 Gemini) with a field emission gun operating at 10 kV. The electrode's structure and phase were investigated by powder X-ray diffraction (XRD) using a Philips's powder diffractometer equipped with Cu kα radiation running at a voltage of 45 kV and a current of 40 mA. The optical properties were analysed by the UV-Vis spectrophotometer (PerkinElmer Lambda 900).

2.6 Electrochemical Characterisation

Electrochemical measurements were carried out using an Autolab potentiostat (Metrohm) (Autolab PGSTAT204). The electrochemical properties of the screen-printed electrodes were investigated in a three-electrode configuration consisting of silver reference electrode, a carbon counter electrode, and a working electrode of ZnO/α-Fe_2O_3NPs. The supporting electrolyte was a 50 µL of 1 M KOH solution that contained arsenic. All measurements were performed at room temperature in a conventional fume hood.

3 Results and Discussions

3.1 Morphological Analysis

The morphologies of the different composite materials, including 2.5 wt% F, 5 wt% F, 7.5 wt% F, 2.5 wt% Z, 5 wt% Z, 7.5 wt% Z and 2.5 wt% ZF, were investigated using a SEM (Figure 2). The surface of the 2.5 wt% F, 5 wt% F and 7.5 wt% F materials exhibited a spherical shape with a particle size less than 50 nm (Figures 2(a) to 2(c)). For the 2.5 wt% Z, 5 wt% Z and 7.5 wt% Z materials, the surface morphology also showed a spherical shape with a slightly larger particle size less than 100 nm (Figures 2(d) to 2(f)). The 2.5 wt% Z was composited with the 2.5 wt% F to form the 2.5 wt% ZF composite. This resulted in a composite material with an approximate thickness of 28.38 µm for the 2.5 wt% Z and 17.56 µm for the 2.5 wt% F (Figures 2(g) and 2(h)). The modification of the 2.5 wt% F onto the surface of the 2.5 wt% Z is suitable for further electrochemical sensing of As^{5+} detection.

3.2 Optical Properties

The UV-visible absorption spectra of bare SPCE, 2.5 wt% F, 5 wt% F, 7.5 wt% F, 2.5 wt% Z, 5 wt% Z and 7.5 wt% Z were investigated. The results showed that the absorption edge was observed at about 395 nm to 400 nm as shown in Figure 3(a). The 2.5 wt% ZF shows an obvious red shift compared to 2.5 wt% Z. With increasing the α-Fe_2O_3NPs layer thickness in the nanocomposite, it has been determined that the 2.5 wt% ZF have higher absorption in the visible light compared to 2.5 wt% Z. The band gap energy of the sample was calculated by using $E_g = 1240/\lambda$ onset (nm), where λ onset is the absorption onset wavelength [28]. The E_g values of 2.5 wt% Z and 2.5 wt% ZF samples were therefore estimated to be about 3.20 eV and 3.18 eV, as shown in Figure 3(b). The 2.5 wt% ZF band gap energy is lower than the 2.5 wt% Z sample.

3.3 XRD Analysis

The XRD was carried out to study the crystal structure of the fabricated electrode materials as revealed in Figure 4. The XRD pattern of bare SPCE, 2.5 wt% F, 2.5 wt% Z, 5 wt% F, 5 wt% Z, 7.5 wt% F and 7.5 wt% Z is shown in Figure 4(a); in which the 2θ diffraction peaks were well matched with the standard JCPDS card (JCPDS No: 00-036-1451) with 2θ diffraction peaks at 31.70°, 34.40°, 36.22° and 47.60° corresponding to the (100), (002), (101) and (102) reflection plane of the ZnO NPs. The diffraction peak at 35.60° which was well matched with the standard JCPDS card No: 00-033-0664 and was attributed to the (110) plane of the α-Fe_2O_3NPs (as shown in Figure 4(b)). The results indicate that 2.5 wt% of ZF has been produced successfully as intended.

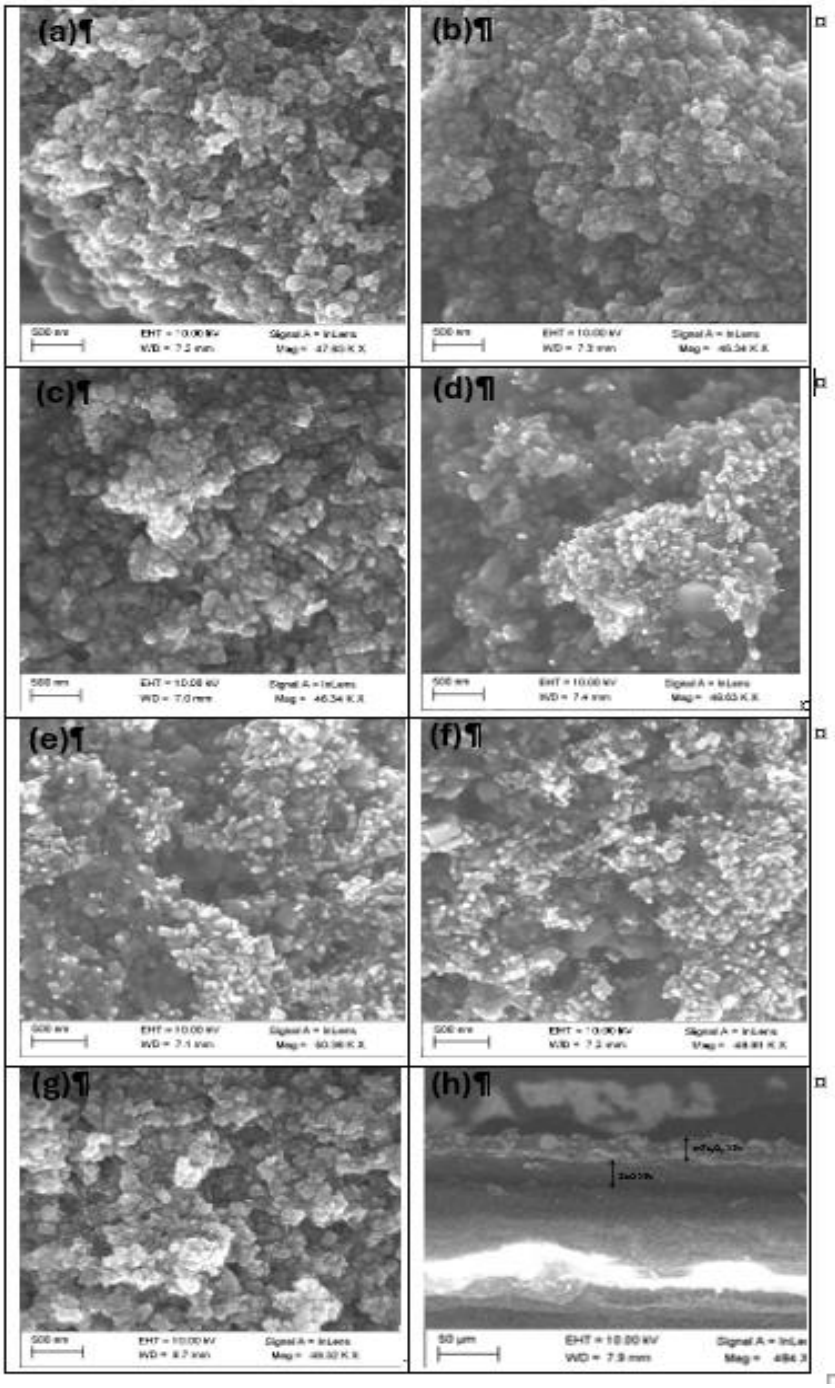

Figure 2: SEM images of (a) 2.5 wt% F, (b) 5 wt% F (c) 7.5 wt% F, (d) 2.5 wt% Z (e) 5 wt% Z, (f) 7.5 wt% Z, (g) 2.5 wt% ZF and cross section of (h) 2.5 wt% ZF

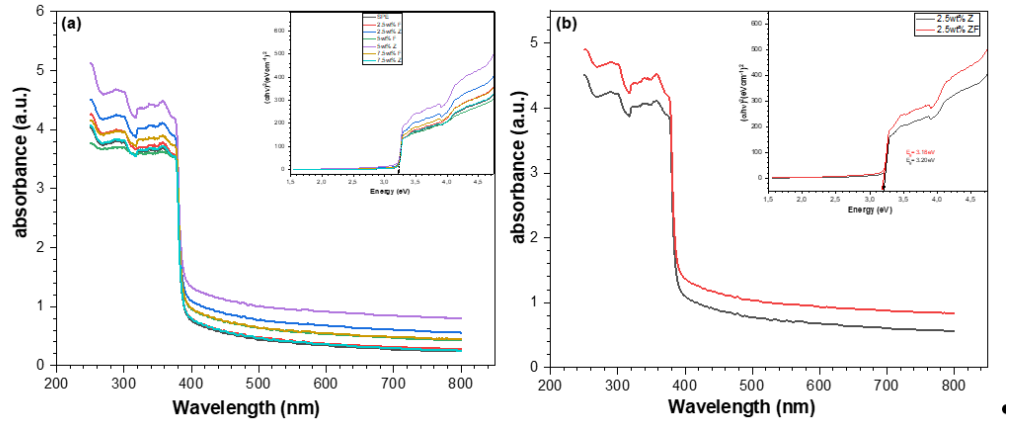

Figure 3: UV-vis absorption spectra of (a) bare of SPCE, 2.5 wt% F, 5 wt% F, 7.5 wt% F, 2.5 wt% Z, 5 wt% Z and 7.5 wt% Z, and (b) 2.5 wt% Z and 2.5 wt% ZF

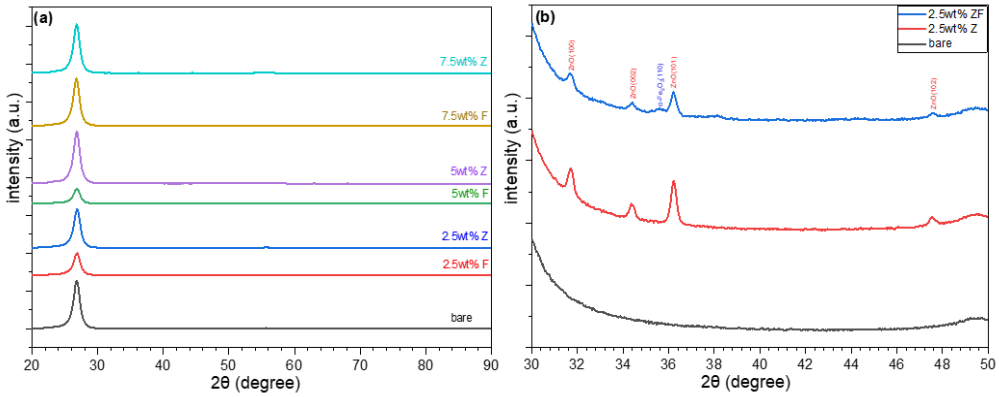

Figure 4: XRD patterns of (a) bare of SPCE, 2.5 wt% F, 5 wt% F, 7.5 wt% F, 2.5 wt% Z, 5 wt% Z and 7.5 wt% Z, and in (b) bare SPCE, 2.5 wt% Z and 2.5 wt% ZF

3.4 Electrochemical Characterisation

The electrochemical performance of the 2.5 wt% F, 5 wt% F, 7.5 wt% F, 2.5 wt% Z, 5 wt% Z and 7.5 wt% Z was studied by LSV. The measurements parameters were carried out ranging from 0.0 V to 0.4 V at a scan rate of 100 mV/s in 50 µL of 1 M KOH electrolyte. The results are shown in Figure 5. The LSV profile with 50 µL of 1 M KOH solution for the 2.5 wt% F, 5 wt% F, 7.5 wt% F, 2.5 wt% Z, 5 wt% Z and 7.5 wt% Z which use different concentration of the α-Fe_2O_3NPs and ZnO NPs show that the peak current is higher for the 2.5 wt% F and 2.5 wt% Z as shown in Figures 5(a) and 5(b). As shown in Figure 5(c), after deposition of the 2.5 wt% F on the 2.5 wt% Z, the

2.5 wt% ZF was higher than both the 2.5 wt% F and 2.5 wt% Z. In addition, the LSV response of 2.5 wt% ZF electrode was measured in 1 M KOH solution at different scan rates from 20 to 100 $mV.s^{-1}$, as shown in Figure 5(d). The LSV response of the 2.5 wt% ZF electrode indicates that the stripping current increases when the value of the arsenic concentration is increased, as shown in Figure 6(a). The calibration plot was found to be linear over a concentration range of 0 to 50 µg /L of As^{5+} and from the calibration curve the regression equation extracted and was found to be $y = 0.15237x + 0.76571$ ($R^2 = 0.996$), as shown in Figure 6(b).

These results indicate that the detection of As^{5+} in an aqueous solution has efficiently been achieved. The lower limit of detection (LOD) was further determined by using the equation of $LOD = 3\sigma/S$, where σ is the standard deviation of the calibration curve that contains samples in the measurements range ($n = 3$), and S is the slope of the calibration curve [29]. The LOD was calculated to be 2.7 ppb, which is lower than the maximum allowed value of 10 ppb by the WHO [9], [30], [31]. The LOD value of the 2.5 wt% ZF electrode was found to be 2.7 ppb, which is also comparable to those reported previously and as presented in Table 1. Although some previous studies have achieved higher sensitivity with lower detection limits, some issues still arise, such as the costly process, the use of toxic materials and complicated fabrication protocols. The repeatability of 2.5 wt% ZF electrode was checked three times by repeating the LSV test in 50 µg /L of As^{5+} solution under optimal condition and the resulting relative standard deviation (RSD) was found to be 14%, which confirms a reasonable stability of the proposed sensor.

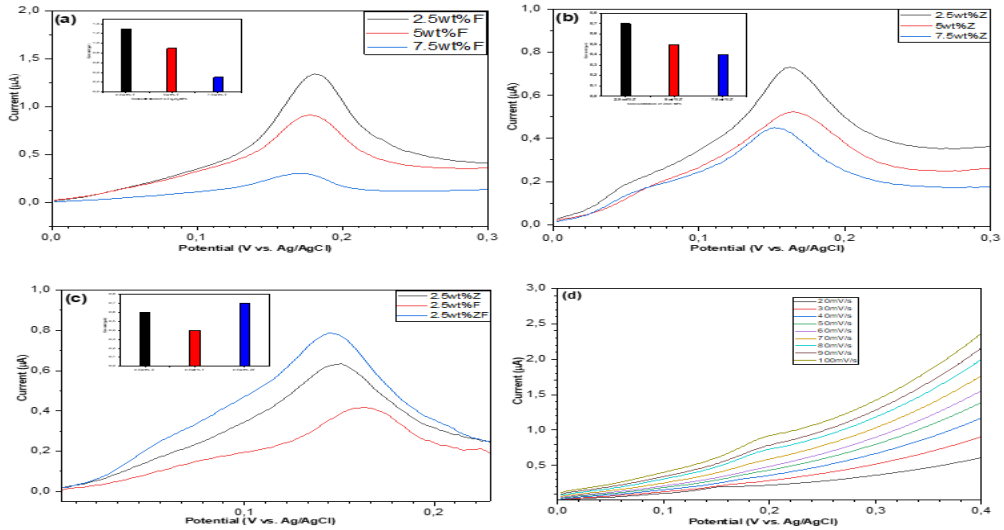

Figure 5: LSV response of the SPCE for different concentrations of (a) 2.5 wt% F, 5 wt% F, 7.5 wt% F (b) 2.5 wt% Z, 5 wt% Z, 7.5 wt% Z, (c) LSV response to 2.5 wt% Z, 2.5 wt% F and 2.5 wt% ZF, and (d) LSV response at different scan rate for the 2.5 wt% ZF electrode

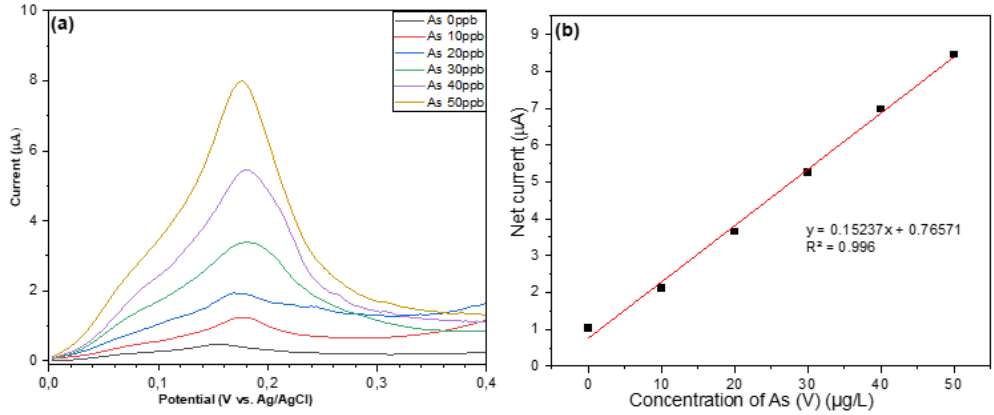

Figure 6: (a) LSV responses of the SPCE for 2.5 wt% ZF electrode towards As^{5+} in a concentration range of 0 to 50 µg/L and (b) the corresponding linear calibration plots of the net current against As^{5+} concentrations

Table 1: Comparative different arsenic detections of electrochemical sensors in previous studies

Electrode	Technique	Modification method	LDR (µg L^{-1})	LOD (ppb)	Ref.
Ag/SPCE	SWASV	Electrodeposition	10–80	8.4	[32]
Fe_3O_4/Au NPs/GCE	SWASV	Drop casting	1–100	0.22	[33]
Fe_3O_4/Co_3S_4/SPCE	SWASV	Drop casting	1–100	0.691	[34]
AuNPs/SiNPs/SPCE	LSASV		10–100	5.6	[35]
ZnONRs/Ni-foam/α-Fe_2O_3NPs	CV	Hydrothermal	10–50	4.12	[36]
ZnO/α-Fe_2O_3NPs/SPCE (2.5 wt% ZF)	LSV	Drop casting	10–50	2.7	This study

3.5 Sensing Mechanism

The energy band structure electrochemical of As^{5+} detection by ZnO/α-Fe_2O_3NPs/SPCE electrode is presented in Figure 7(a). The conduction band (CB) and valence band (VB) of α-Fe_2O_3 (0.1 eV and 2.4 eV) are more negative than those of ZnO (−0.34 eV and 2.86 eV), in which the electrons are transferred from the conduction band of the α-Fe_2O_3 to ZnO. Meanwhile, the holes of the ZnO in the valence band migrate to the valence band of the α-Fe_2O_3. The electrons and holes which migration and separation are achieved at the heterojunction interface. When the ZnO/α-Fe_2O_3, which is an n-n heterojunction, has contact with the electrolyte, electrons at the Fermi level align to attain equilibrium. The Fermi level in the α-Fe_2O_3 is located in between its CB and VB, which is approximately 1.24 eV. The Fermi level of n-typical semiconductor generally

lies at the bottom of the CB by ca. 0.1–0.2 eV [37]. The Fermi level of the α-Fe_2O_3 is at 1.24 eV as a typical n-type semiconductor. When the ZnO and α-Fe_2O_3 are attended together that their Fermi levels align, it will appear at 1.25 eV.

The sensing mechanism for boosting the stripping signal for As^{5+} analysis is shown in Figure 7(b). The absorption of ZnO/α-Fe_2O_3 with oxygen vacancies and the freely diffusing As^{5+} in the solution were dispersed onto the ZnO/α-Fe_2O_3NPs/SPCE surface. The As^{5+} species can then be chemically reduced to H_3AsO_3 during the electrochemical performance of the electrode. These reactions can be coupled to an electrochemical step in the H_3AsO_3 which is reduced to zero-valent arsenic on the ZnO/α-Fe_2O_3NPs/SPCE surface. Zero-valent arsenic were adsorbed onto the electrode surface, and the stronger stripping peak signal was obtained later [36].

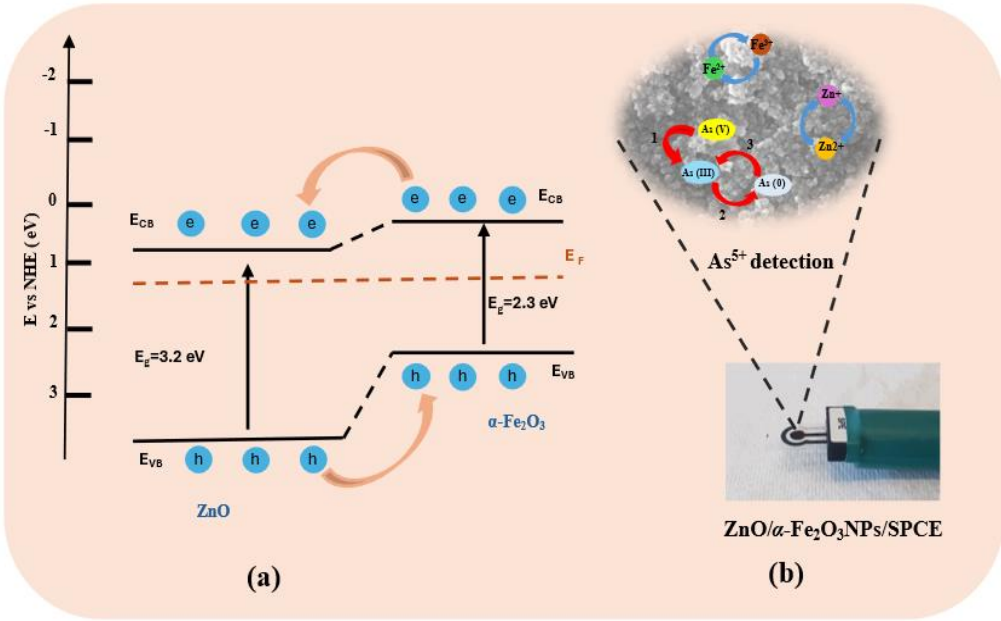

Figure 7: (a) Equilibrium energy band structure diagram of ZnO/α-Fe_2O_3NPs/SPCE and (b) showing the sensing mechanism

3.6 Selectivity and Effect of Interfering Species

The selectivity of the proposed sensor is an important parameter for real aqueous sample applications. The fabricated electrodes are evaluated in the presence of potentially interfering elements, including Ag^+, Cd^{2+}, Fe^{3+}, K^+ and Zn^{2+}, under similar experimental conditions that have been used for the determination of the As^{5+} in the dispersion of the 2.5 wt% ZF NPs electrode. The interference of metal ions was investigated using different metal salts; KCl, $AgNO_3$, Cd $(NO_3)_2$ $4H_2O$, Zn $(NO_3)_2$ $6H_2O$ and Fe $(NO_3)_3$ $9H_2O$ were used. The concentration of metal salts was maintained at 50 µg/L in 50 µL

of deionised water, with 1 M KOH solution. It was observed that, in the presence of interfering metal ions, the signal was 10 times smaller than that of the As^{5+}. Consequently, no significant interference could be observed as shown in Figure 8. This 2.5 wt% ZF electrode can be used successfully for detection of As^{5+}, as Figure 8 shows that the sensor has low interference due to other common metal ions available in drinking water. The 2.5 wt% ZF electrode therefore has excellent selectivity for As^{5+} detection and is a promising structure for future demonstrations of a robust sensor.

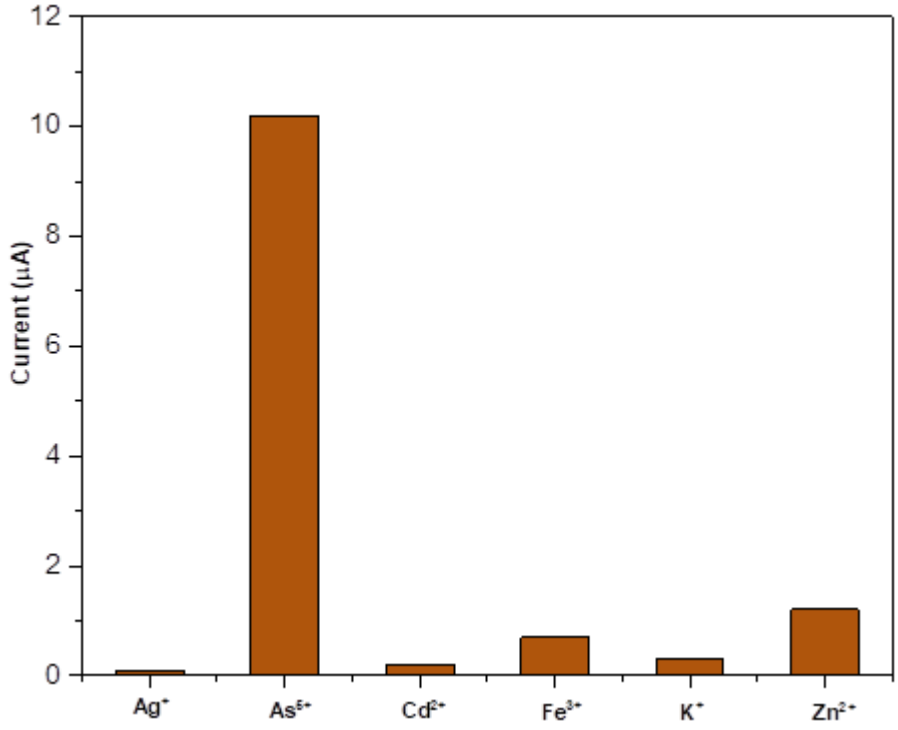

Figure 8: Effect of interference in the presence of different metal ions under similar experimental conditions (50 ppb) that have been used for detection of As^{5+} in the dispersion of 2.5 wt% ZF electrode

4 Conclusion

In summary, screen-printed and drop-casting methods were used to demonstrate the ZnO/α-Fe_2O_3NPs/SPCE sensor for As^{5+} detection characterised by LSV. The fabrication of the ZnO/α-Fe_2O_3NPs/SPCE was successfully achieved via the drop-casting method with optimisation towards the electrode performance. The ZnO/α-Fe_2O_3NPs/SPCE (2.5 wt% ZF) electrode showed the best results, which demonstrated the highest reduction current towards As^{5+} detection compared to other samples. The electrode showed attractive sensing performed toward As^{5+} with regard to the good

sensitivity with LOD value, which was found to be 2.7 ppb. This value is lower than the highest recommended allowed limit for arsenic in drinking water as suggested by the WHO. In addition, the demonstrated sensing electrode showed good selectivity. Our results indicate that the ZnO/α-Fe_2O_3NPs/SPCE (2.5 wt% ZF) electrode is a promising material to use because of its electrocatalytic activities towards As^{5+} detection in drinking water.

6 Author Statement

SM synthesised the electrode, carried out the characterisations, analysed the results and wrote the first draft of the manuscript. MN and OM worked on the manuscript's editing.

7 Acknowledgements

The authors acknowledge the financial support from the Department of Science and Technology at the Linköping University, the International Science Programme at Uppsala University and the Swedish International Development Cooperation Agency.

References

[1] J. H. T. Luong, E. Lam and K. B. Male, "Recent advances in electrochemical detection of arsenic in drinking and ground waters," *Anal. Methods*, vol. 6, no. 16, pp. 6157–6169, 2014, doi: 10.1039/C4AY00817K.

[2] W. R. Cullen and K. J. Reimer, "Arsenic speciation in the environment," *Chem. Rev.*, vol. 89, no. 4, pp. 713–764, Jun. 1989, doi: 10.1021/cr00094a002.

[3] J. M. Zen, P. Y. Chen and A. S. Kumar, "Flow Injection Analysis of an Ultratrace Amount of Arsenite Using a Prussian Blue-Modified Screen-Printed Electrode," *Anal. Chem.*, vol. 75, no. 21, pp. 6017–6022, Sept. 2003, doi: 10.1021/ac0301649.

[4] S. Nellaiappan, K. C. Pillai and A. S. Kumar, "Flow-injection analysis coupled with electrochemical detection of poisonous inorganic arsenic(III) species using a gold nanoparticle/carbon nanofiber/chitosan chemically modified carbon screen printed electrode in neutral pH solution," *Anal. Methods*, vol. 10, no. 7, pp. 799–808, 2018, doi: 10.1039/C7AY02655B.

[5] H. Dharmagunawardhane, "Arsenic Contamination in Cambodia: A Status Review," *2nd Int. Symp. Conserv. Manag. Trop. Lakes*, no. November, 2018.

[6] J. J. Costa and M. Maniruzzaman, "Detection of Arsenic Contamination in Drinking Water using Color Sensor," *2018 Int. Conf. Adv. Electr. Electron. Eng. ICAEEE 2018*, pp. 1–4, 2018, doi: 10.1109/ICAEEE.2018.8642980.

[7] Z. Xie *et al.*, "Electrochemical Detection of As(III) by a rGO/Fe_3O_4-modified Screen-Printed Carbon Electrode," *Anal. Sci.*, vol. 32, no. 10, pp. 1053–1058, Oct. 2016, doi: 10.2116/analsci.32.1053.

[8] S. Aredes, B. Klein and M. Pawlik, "The removal of arsenic from water using natural iron oxide minerals," *J. Clean. Prod.*, vol. 60, pp. 71–76, Dec. 2013, doi: 10.1016/j.jclepro.2012.10.035.

[9] S. Dutta *et al.*, "A luminescent cationic MOF for bimodal recognition of chromium and arsenic based oxo-anions in water," *Dalt. Trans.*, vol. 50, no. 29, pp. 10133–10141, 2021, doi: 10.1039/D1DT01097B.

[10] J. J. Wouters *et al.*, "Performance of SiO_2, ZrO_2, TiO_2, Al_2O_3 or Fe_2O_3 Coatings on Ti Electrodes for Arsenic (V) Detection Utilizing Electrochemical Impedance Spectroscopy," *J. Electrochem. Soc.*, vol. 165, no. 2, pp. B34–B47, Jan. 2018, doi: 10.1149/2.0611802jes.

[11] D. Lu *et al.*, "Simultaneous voltammetric detection of cadmium(II), arsenic(III), and selenium(IV) using gold nanostar-modified screen-printed carbon electrodes and modified Britton-Robinson buffer," *Anal. Bioanal. Chem.*, vol. 412, no. 17, pp. 4113–4125, Apr. 2020, doi: 10.1007/s00216-020-02642-4.

[12] S. Kempahanumakkagari *et al.*, "Nanomaterial-based electrochemical sensors for arsenic – A review," *Biosens. Bioelectron.*, vol. 95, pp. 106–116, Sept. 2017, doi: 10.1016/j.bios.2017.04.013.

[13] A. O. Idris *et al.*, "Nanogold modified glassy carbon electrode for the electrochemical detection of arsenic in water," *Russ. J. Electrochem.*, vol. 53, pp. 170–177, Mar. 2017, doi: 10.1134/S1023193517020082.

[14] J. P. Metters, R. O. Kadara and C. E. Banks, "New directions in screen printed electroanalytical sensors: an overview of recent developments," *Analyst*, vol. 6, pp. 1067–1076, 2011, doi: 10.1039/c0an00894j.

[15] A. D. Ambaye *et al.*, "Screen-printed electrode system based on carbon black/copper-organic framework hybrid nanocomposites for the electrochemical detection of nitrite," *Mater. Today Commun.*, vol. 35, p. 105567, Jun. 2023, doi: 10.1016/j.mtcomm.2023.105567.

[16] S. Z. Bas *et al.*, "A lab-made screen-printed sensing strip for sensitive and selective electrochemical detection of butylated hydroxyanisole," *Lab. Chip*, vol. 6, pp. 1664–1673, 2023, doi: 10.1039/D3LC00060E.

[17] K. Arshak, I. Gaidan and L. Cavanagh, "Screen-Printed Fe2O3/ZnO thick films for gas sensing applications," *J. Microelectron. Elect. Pkg.*, vol. 2, no. 1, pp. 25–39, Jan. 2005, doi: 10.4071/1551-4897-2.1.25.

[18] A. Geto *et al*., "Electrochemical determination of bentazone using simple screen-printed carbon electrodes," *Environ. Int*., vol. 129, pp. 400–407, Aug. 2019, doi: 10.1016/j.envint.2019.05.009.

[19] M. A. Belal *et al*., "Advances in gas sensors using screen printing," *J. Mater. Chem. A*, vol. 8, pp. 5447–5497, 2025, doi: 10.1039/D4TA06632D.

[20] D. Antuña-Jiménez *et al*., "Screen-Printed Electrodes Modified with Metal Nanoparticles for Small Molecule Sensing," *Biosensors*, vol. 10, no. 2, pp. 1–22, Feb. 2020, doi: 10.3390/bios10020009.

[21] M. Won *et al*., "Fabrication of a Fully Printed Ammonia Gas Sensor Based on ZnO/rGO Using Ultraviolet–Ozone Treatment," *Sensors*, vol. 24, no. 5, pp. 1–12, Mar. 2024, doi: 10.3390/s24051691.

[22] S. Touba and S. Kimiagar, "Enhancement of sensitivity and selectivity of α-Fe_2O_3 nanorod gas sensors by ZnO nanoparticles decoration," *Mater. Sci. Semicond. Process*., vol. 102, p. 104603, Nov. 2019, doi: 10.1016/j.mssp.2019.104603.

[23] K. Fan *et al*., "Atomic layer deposition of ZnO onto Fe_2O_3 nanoplates for enhanced H_2S sensing," *J. Alloys Compd*., vol. 698, pp. 336–340, Mar. 2017, doi: 10.1016/j.jallcom.2016.12.203.

[24] R. Ahmad, M. S. Ahn and Y. B. Hahn, "A Highly Sensitive Nonenzymatic Sensor Based on Fe_2O_3 Nanoparticle Coated ZnO Nanorods for Electrochemical Detection of Nitrite," *Adv. Mater. Interfaces*, vol. 4, no. 22, pp. 1–9, Nov. 2017, doi: 10.1002/admi.201700691.

[25] Y. K. Hsu, Y. C. Chen and Y. G. Lin, "Novel ZnO/Fe_2O_3 Core-Shell Nanowires for Photoelectrochemical Water Splitting," *ACS Appl. Mater. Interfaces*, vol. 7, no. 25, pp. 14157–14162, Jun. 2015, doi: 10.1021/acsami.5b03921.

[26] Y. Liu *et al*., "Preparation and photocatalytic activity of ZnO/Fe_2O_3 nanotube composites," *Mater. Sci. Eng. B*, vol. 194, pp. 9–13, Apr. 2015, doi: 10.1016/j.mseb.2014.12.021.

[27] N. Kodan, M. Ahmad and B. R. Mehta, "Enhanced photoelectrochemical response and stability of hydrogenated ZnO nanorods decorated with Fe_2O_3 nanoparticles," *J. Alloys Compd*., vol. 845, p. 155650, Dec. 2020, doi: 10.1016/j.jallcom.2020.155650.

[28] M. Sabonian and K. Mahanpoor, "Preparation of ZnO nanocatalyst supported on todorokite and photocatalytic efficiency in the reduction of chromium (VI) pollutant from aqueous solution," *Russ. J. Commun*., vol. 3, no. 3/4, pp. 1717–1722, 2010.

[29] M. Nazari, S. Kashanian and R. Rafipour, "Laccase immobilization on the electrode surface to design a biosensor for the detection of phenolic compound such as catechol," *Spectrochim. Acta Part A: Mol. Biomol. Spectrosc*., vol. 145, pp. 130–138, Jun. 2015, doi: 10.1016/j.saa.2015.01.126.

[30] Y. Sayato, “WHO Guidelines for Drinking-Water Quality,” *Eisei kagaku*, vol. 35, no. 5, pp. 307–312, 1989, doi: 10.1248/jhs1956.35.307.

[31] P. G-Saiz *et al*., “Metal-Organic Frameworks for Dual Photo-Oxidation and Capture of Arsenic from Water,” *ChemSusChem*, vol. 17, no. 24, p. 202400592, Dec. 2024, doi: 10.1002/cssc.202400592.

[32] S. P. M. Cortés *et al*., “Square Wave Anodic Stripping Voltammetry Determination of Arsenic (III) onto Carbon Electrodes by Means of Co-deposition with Silver,” *J. Mex. Chem. Soc*., vol. 62, no. 2, pp. 314–322, 2018, doi: 10.29356/jmcs.v62i2.430.

[33] M. Sedki *et al*., “Linker-Free Magnetite-Decorated Gold Nanoparticles (Fe_3O_4-Au): Synthesis, Characterization, and Application for Electrochemical Detection of Arsenic (III),” *Sensors*, vol. 21, no. 3, pp. 1–13, Jan. 2021, doi: 10.3390/s21030883.

[34] H. Q. Huang *et al*., “Noble-metal-free Fe_3O_4/Co_3S_4 nanosheets with oxygen vacancies as an efficient electrocatalyst for highly sensitive electrochemical detection of As(III),” *Anal. Chim. Acta*, vol. 1189, p. 339208, Jan. 2022, doi: 10.1016/j.aca.2021.339208.

[35] S. Ismail *et al*., “Development of Electrochemical Sensor Based on Silica/Gold Nanoparticles Modified Electrode for Detection of Arsenite,” *IEEE Sens. J*., vol. 20, no. 7, pp. 3406–3414, Apr. 2020, doi: 10.1109/JSEN.2019.2953799.

[36] S. Ngok *et al*., “Fabrication of an α-Fe_2O_3 NP-modified ZnO NRs/Ni-foam nanocomposite electrode for electrochemical detection of arsenic in drinking water,” *RSC Adv*., vol. 51, pp. 37725–37736, 2024, doi: 10.1039/D4RA07509A.

[37] Y.-L Li *et al*., “Fabrication of core-shell $BiVO_4$@Fe_2O_3 heterojunctions for realizing photocatalytic hydrogen evolution via conduction band elevation,” *Mater. Des*., vol. 187, p. 108379, Feb. 2020, doi: 10.1016/j.matdes.2019.108379.